Spectrochimica Acta Part A: Molecular and Biomolecular Spectroscopy 304 (2024) 123423

Contents lists available at ScienceDirect

Spectrochimica Acta Part A:
Molecular and Biomolecular Spectroscopy

journal homepage: www.journals.elsevier.com/spectrochimica-acta-part-a-molecular-and-biomolecular-spectroscopy

A comprehensive investigation on the interaction between jaceosidin, baicalein and lipoxygenase: Multi-spectroscopic analysis and computational study

Zeru Xu [a], Hongying Du [a,b,*], Anne Manyande [c], Shanbai Xiong [a]

[a] Key Laboratory of Environment Correlative Dietology, Ministry of Education, College of Food Science and Technology, Huazhong Agricultural University, Wuhan, Hubei, PR China
[b] Department of Food Science and Engineering, College of Light Industry and Food Engineering, Nanjing Forestry University, Nanjing 210037, PR China
[c] School of Human and Social Sciences, University of West London, Middlesex TW8 9GA, UK

HIGHLIGHTS

- JSD and BCL have been screened out as the potential LOX inhibitors.
- JSD and BCL binding to LOX lead to static fluorescence quenching.
- The secondary structure changes of LOX was changed with the interaction of JSD/BCL.
- Hydrogen bond and van der Waals force play a major role in the binding to LOX.

GRAPHICAL ABSTRACT

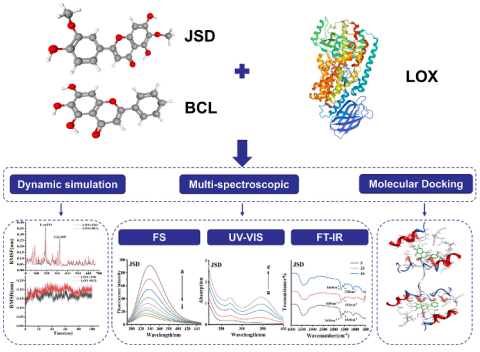

ARTICLE INFO

Keywords:
Lipoxygenase (LOX)
Jaceosidin
Baicalein
Interaction
Multi-spectrum
Molecular dynamics simulation

ABSTRACT

Lipoxygenase (LOX) has the harmful effect of accelerating lipid oxidation, and polyphenols have the inhibitory effect on lipoxygenase. However, there were rare researches investigated on the interactions between polyphenols and LOX. In this study, the binding mechanisms between polyphenols (Jaceosidin-JSD and baicalein-BCL) and LOX were investigated by multi-spectroscopic analysis and computational study. Both JSD and BCL binding to LOX resulted in static fluorescence quenching, and the complexes of JSD-LOX and BCL-LOX were built at a molar ratio of 1:1, respectively. The binding constants of LOX-JSD (72.18×10^5 L/mol at 298 K) and LOX-BCL (12.43×10^5 L/mol at 298 K) indicated that LOX had stronger binding affinity to JSD compared to BCL. Compared with BCL-LOX, the JSD-LOX system formed more hydrogen bonds which ensured a stronger bond between JSD and LOX. The studies in molecular dynamics also demonstrated that the JSD-LOX complex is more stable, and the addition of JSD is more conducive to the complex formation. The current study provides some new insights for the study on the inhibition of lipid oxidation and affords a new strategy for the discovery of novel food preservatives.

* Corresponding author at: Key Laboratory of Environment Correlative Dietology, Ministry of Education, College of Food Science and Technology, Huazhong Agricultural University, Wuhan, Hubei, PR China.
E-mail address: hydu@njfu.edu.cn (H. Du).

https://doi.org/10.1016/j.saa.2023.123423
Received 5 December 2022; Received in revised form 11 August 2023; Accepted 16 September 2023
Available online 18 September 2023

1. Introduction

Lipoxygenase (LOX, EC 1.13.11.12) is a type of non-heme iron containing protein, which oxidizes unsaturated fatty acids and fatty acid esters with a 1,4-cis, *cis*-pentadiene structure and converts them to hydroperoxides [28]. In the catalytic cycle of LOX, the activation of the diene by Fe^{3+} in the enzyme active site, with an intermediate bis (allyl) radical (or similar iron coordination) species reacting directly with dioxygen,the peroxide radicals are reduced by Fe^{2+} to form hydroperoxides, and Fe2+ is converted to Fe^{3+} which continues to participate in the reaction [27]. Due to the high reactivity of free radicals produced by the breakdown of hydroperoxides, they are able to initiate free radical chain reactions with biomolecules, such as proteins, lipids, and DNA, and destroy the components of the organism, thereby damaging the body tissues.

LOX activity usually deteriorates the quality of aquatic products and it induces a variety of physicochemical reactions which should not be ignored during the storage. It has found that the increase of fishy odor was regulated by LOX-induced oxidation during Nile tilapia preservation [32]. LOX in sardine mince can trigger the oxidation of PUFAs and produces labile hydroperoxides in fish tissues, which induces aggregation of proteins, reduction of insolubility and the formation of colored complexes [39]. Endogenous LOX of mussel (*Mytilus edulis*) promotes the degree of hydrolysis and oxidation of lipids during the refrigeration, which leads to the lipid nutrient loss and fatty acid composition changes [49]. Therefore, it is very necessary to inhibit the activity of LOX for aquatic product storage.

Plant polyphenols have strong antioxidant capacity due to the existence of active phenolic hydroxyl. Many studies have proved that plant polyphenols can reduce LOX activity. Green tea polyphenols have potent free radical quenching effects, and their antioxidant activity is partly attributable to specific structural features that can interfere with the LOX pathway [17]. Chlorogenic acid can inhibit the endogenous LOX enzyme activity of grass carp, reduce the level of lipid oxidation during storage [4]. Baicalein is an effective inhibitor of lipoxygenase, which is one of the reasons why it inhibits the oxidation process [34].Currently, many biochemical investigations have found that phenolic compounds are LOX inhibitors, and they have the ability to scavenge free radicals and/or chelate iron [21]. Sesamol inhibited the activity of lipoxygenase by preventing the conversion of inactive LOX (Fe^{2+}) to active LOX (Fe^{3+}) and scavenging free radicals [44]. Curcumin also competitively inhibited soybean lipoxygenase by affecting the active site iron [2]. As human platelet 12-LOX and human reticulocyte 15-LOX, baicalin can reduce trivalent LOX with catalytic activity to an inactive ferrous form, which is oxidized to baicalin free radicals [10,35]. Most studies focus on the inhibition mechanism of polyphenols on LOX activity, but the research on the interaction between polyphenols and LOX is not very sufficient. In recent years, some studies have further explored the interaction between polyphenols and lipoxygenase through multi-spectroscopy and molecular simulation [25,8]. Our research has found that the inhibitory activity of baicalein and jaceosidin on lipoxygenase is strong. However, the interaction between polyphenols and LOX has rarely been reported. So a comprehensive study of the interaction between polyphenols and LOX is still needed.

Jaceosidin (JSD) is a flavonoid compound derived from the herb of Artemisia vestita wall, and it exhibits anti-cancer effects based on some cytotoxicity studies [24,40]. Baicalein (BCL) is a flavonoid derived from the roots of Scutellaria baicalensis Georgi (a traditional medicinal herb), which has a variety of pharmacological activities such as antioxidant, antiviral, anti-bacterial, anti-inflammatory, antiallergic and so on [3,37]. In this study, JSD and BCL (the molecular structures of them are shown in Table S1) were used to interact with LOX, and explore the corresponding binding mechanism. Soybean lipoxygenase was used as a model enzyme. At present, the main methods to study the interaction between proteins and small molecules are multispectral method and molecular docking [22]. In addition, dynamic simulation plays an important role in studying the stability and dynamic behavior of proteins and small molecules. The quenching mechanism, binding parameters, thermodynamic parameters, conjugation model, binding sites, and conformational changes JSD-LOX and BCL-LOX systems were investigated using multi-spectroscopic and computational study. It might provide some new insights for the study on the inhibition of lipid oxidation and the discovery of novel food preservatives.

2. Materials and methods

2.1. Chemicals

Lipoxygenase (EC 1.13.11.12, 10 u/mg protein, 108 kDa), and all polyphenols (purity greater than 98 %) were provided by Shanghai Yuanye Biological Technology Co., Ltd. (Shanghai, China). The Nitrophenyl butyrate (4-NPB, purity $\geq$ 98 %) was provided by Shanghai Yuanye Biological Technology Co., Ltd. All reagents and chemicals used in the present study were of analytical grade, and polyphenol solutions were ready to be prepared before use to avoid autoxidation.

2.2. Inhibition assays

LOX's activity was assayed at 234 nm using a UV–vis spectrophotometer (MAPADA, Shanghai, China) according to a former method with modifications [14]. The substrate solution of LOX was prepared by dissolving 0.27 mL linoleic acid and 0.25 mL Tween-20 in boric acid buffer (10 mL, 0.2 mol/L, pH = 9.0), the pH value was adjusted to 9.0 with 1 mol/L NaOH. Finally, the above solution was adjusted to 500 mL with borate buffer (10 mL, 0.2 mol/L, pH = 9.0) and used as a substrate. Subsequently, fixed concentration of LOX (1 mL, 0.4 mg/mL) was mixed with polyphenols (0–70 μM) and substrate linoleic acid (0.25 mL, 2 mM), then the mixture is made up to 15 mL with borate buffer (0.2 mol/L, pH = 9.0), and the mixed solution was equilibrated for 10 min at 37 °C. One minute after the reaction, the absorbance at 234 nm was recorded. One unit of LOX's activity was defined as an increase of absorbance at 234 nm of 0.001 per min under assay condition.

2.3. Fluorescence measurements

LOX solution (0.1 mg/mL) was mixed with polyphenol solutions (0, 5.0, 10.0, 15.0, 20.0, 25.0, 30.0, 35.0, 40.0 $\times$ 10^{-6} M), and finally a boric acid buffer (0.2 mol/L, pH = 9.0) was added. The fluorescence spectra of all samples were collected on F-4500 fluorescence spectrometer (Hitachi, Japan). The fluorescence emission spectroscopy was carried out at three different temperatures (298, 304 and 310 K) with an excitation wavelength of 290 nm and a wavelength range of 290–450 nm. The slit widths for the excitation and emission were both adjusted to 5 nm. All solutions were balanced at the set temperature for 30 min before measurement.

2.4. Synchronous fluorescence

The synchronous fluorescence spectra of the LOX and LOX-polyphenols complexes were measured at $\Delta\lambda$ = 15 nm and 60 nm on F-4500 fluorescence spectrometer (Hitachi, Japan) with 5/5 nm slit widths (n = 3/group). The settings were as follows: the voltage is 400 V, the scanning speed is 1200 nm/min, and the scanning range is 260 nm–340 nm.

2.5. UV–vis measurements

UV–vis absorption were measured using a UV-2600 spectrophotometer (UNIC, China).The solutions contained LOX solution (1 mg/mL), relative boric acid buffer (0.2 mol/L, pH = 9.0) and various doses of polyphenol solutions (0, 10, 20, 30, 40 $\times$ 10^{-6} mol/L). The absorption spectra were recorded ranging from 230 to 450 nm (n = 3/group).

2.6. FT-IR measurements

The LOX solution (0.1 mg/mL) was combined with relative boric acid buffer (0.2 mol/L, pH = 9.0) and polyphenol solutions (0, 20, 40 × 10^{-6} M), and then all samples are freeze-dried. The FT-IR spectra of the samples were gauged in the range of 4000 to 500 cm^{-1} with 64 scans and 4 cm^{-1} resolutions by a Nicolet470 FT-IR spectrometer (Nicolet, USA) in a KBr pellet (n = 3/group). A background spectral scan was performed before each measurement.

2.7. Particle size measurement

The particle size and polydispersity index (PDI) were measured on the Malvern Zetasizer Nano ZS (Zetasizer Nano ZS, Malvern Instruments, Worcestershire, UK). The solutions containing LOX solution (0.1 mg/mL), polyphenol solutions (ranging from 0 to 4 × 10^{-6} M, stepped by 1 × 10^{-6} M) and relative boric acid buffer (0.2 mol/L, pH = 9.0). All samples were determined, and the experiment repeated 3 times for each group.

2.8. Observation with atomic force microscopy (AFM)

The LOX (0.1 mg/mL) or LOX-polyphenols (C_{LOX} = 0.1 mg/mL, $C_{polyphenols}$ = 20.0 × 10^{-6} M) solution was dispersed in absolute ethanol to be transparent, then sonicated for 20 min. The sample solution was dropped on a freshly cleaved flat mica surface until the ethanol dried. AFM measurements were performed in tapping mode using a Dimension edge atomic force microscope at room temperature.

2.9. Molecular docking

The crystallographic structure of LOX with PDB ID: 2P0M was obtained from the Protein Data Bank (PDB: https://www.rcsb.org/). The structures of JSD and BCL were obtained from the PubChem (https://pubchem.ncbi.nlm.nih.gov/). The Fe atom was positioned within the docking box. The center of docking box locates at the Cα atom of L597, and the box size was 30 Å × 30 Å × 30 Å. The extra precision (XP) flexible docking was performed by the Glide module of Schrödinger-Maestro v11.3 [12,13], which is more sophisticated than the SP/HTVS in scoring function [13].

2.10. Molecular dynamics simulation

The molecular dynamics simulation was carried out using GROMACS 2019 (Abraham, et al., 2015) with an Amber's FF03 force field and the force field of LOX were obtained in gromacs code via PDB2GMX tool. The Gaussian09 code [33] was applied to calculate the electrostatic potential of JSD and BCL, and the Antechamber tool in AmberTools [7] was used by employing the RESP [51] charge fitting method. The LOX-JSD and LOX-BCL complexes were put in a solvent environment approximating normal saline (0.15 M NaCl) at a temperature of 300 K in order to reduce the energy for 1000 steps. The reduced system was then brought to equilibrium for 100 ps in the NVT ensemble and then for an additional 100 ps in the NPT ensemble. After then, a manufacturing run lasting 100 ns total was carried out at 300 K with a 2 fs time step. The final 10 ns of steady kinetic trajectories were used to acquire 100 frames of kinetic trajectory files, and the binding free energy for this trajectory was calculated using the MM/PBSA [20] approach.

2.11. Statistical analysis

All the experiments were conducted in triplicate and significant differences between the means ($p < 0.05$) were determined by the one-way ANOVA test. The figures were produced using Origin2020 software.

3. Results and discussion

3.1. Inhibitory activities for lipoxygenase

The inhibition effect of JSD and BCL on LOX activity is displayed in Fig. S1. As shown in Fig. S1, when the concentration of LOX was kept at 0.4 mg/mL, the enzymatic activity of LOX significantly decreased with increasing amounts of JSD and BCL. One-way ANOVA analysis showed that the inhibitor concentrations have significant effects on the inhibition rate of LOX ($p < 0.05$).To compare the inhibitory efficiency of different polyphenols, IC50 values were measured. The IC50 values of JSD and BCL for LOX are 25.32μM and 27.16 μM respectively, suggesting that JSD has a higher LOX inhibitory activity compared with BCL.

3.2. Effect of BCL and JSD on fluorescence emission spectra of LOX

The fluorescence spectroscopy can explore the binding of small molecules to proteins and can reveal some details regarding the binding mechanism, binding constants, and binding sites. As shown in Fig. 1-a1, a significant quenching in the fluorescence intensities of LOX accompanied by a blue shift in the fluorescence emission wavelength (from 339 to 329 nm) was noticed. This phenomenon (the blue shift in fluorescence emission wavelength) indicates a rise in the hydrophobicity around the fluorophore and amino acid residues of LOX when JSD is added. Furthermore, the fluorescence intensities were remarkably decreased without significant changes in the fluorescence emission maximum after the addition of BCL, which demonstrates that BCL has a quenching effect on the intrinsic fluorescence of LOX and forms a stable complex with LOX (Fig. 1-a2).

Similar results were also reported showing that the fluorescence intensity of bovine serum albumin decreased with the addition of butylated hydroxyanisole, and a slight blue shift of 3 nm emerged which indicates that the microenvironment of bovine serum albumin had been changed by butylated hydroxyanisole [15]. The relative fluorescence quenching rates were 76.69 % and 85.04 % when BCL and JSD were added at the highest concentration to LOX respectively, which demonstrates that JSD quenched the intrinsic fluorescence of LOX more easily than BCL.

3.3. Fluorescence quenching mechanisms

Temperature-dependent fluorescence measurements were gauged at three different temperatures (298, 205, and 310 K) to elaborate the quenching mechanism, the fluorescence quenching data were calculated by the well-known Stern-Volmer equation [47].

$$F_0/F = 1 + K_q\tau_0[Q] = 1 + K_{sv}[Q] \quad (2)$$

F_0 is fluorescence intensity of LOX and F are fluorescence intensities of LOX-polyphenols complexes, K_q is the quenching rate constant of biomolecule, τ0 is the average lifetime of a fluorescence molecule (about 10^{-8} s^{-1}), and [Q] is the concentration of the quencher. K_{SV} is the quenching constant ($K_{SV} = K_q\tau_0$).

The fluorescence quenching is usually classified as static quenching (quenching constant is inversely proportional to temperature), dynamic quenching(quenching constant is proportional to temperature), or a combination of the two mechanisms [16]. The linear relationship of F_0/F with BCL and JSD molar concentrations at three different temperatures is displayed in Fig. 1b. The good linear relationship between the F_0/F value and the quencher concentration suggests that the LOX-BCL and LOX-JSD interaction modes are purely static or dynamic mechanisms. As displayed in Table 1, the relationship between the calculated K_{SV} and K_q values and temperature is inverse, and the K_q values are more than 2.0 × 10^{10} L/mol s^{-1}. The findings indicate that the fluorescence quenching mode of LOX by inhibitors is static quenching, which coincides with the findings from a prior investigation on the interaction of myosin and

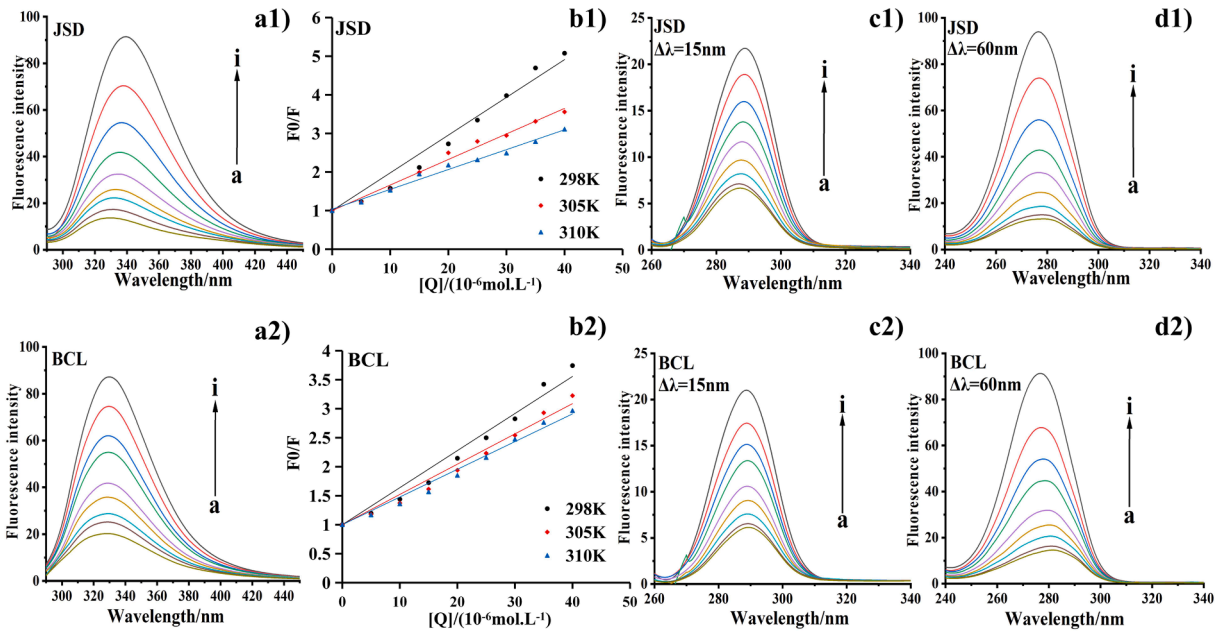

Fig. 1. Fluorescence spectra analysis of the interaction between JSD (a1–d1) or BCL (a2–d2) and LOX. Note: a1 and a2: The fluorescence spectrum of LOX without or with different concentrations of JSD and BCL (a–i) at 298 K; b1 and b2: Stern-Volmer plots for fluorescence quenching; c and d: Synchronous fluorescence spectrum of JDS-LOX and BCL-LOX complex, c-$\Delta\lambda = 15$ nm, d-$\Delta\lambda = 60$ nm. The concentrations of JSD and BCL were 0.00 to 40.00 $\times$ 10^{-6} mol/L, with a concentration gradient of 5 $\times$ 10^{-6} mol/L for curves a–i.

chlorogenic acid [18].

3.4. Binding constant and binding number

For static quenching, the binding constant (K_d) and binding number (n) of LOX–BCL and LOX-JSD systems at 298, 305 and 310 K can be calculated by the logarithmic transformation mode of Stern-Volmer equation.

$$log[(F_0 - F)/F] = logK_a + nlog[Q] \quad (3)$$

The results are displayed in Table 1. The K_d value is the binding constant and it was gained from the slope of the straight line, n is the number of binding sites per protein and it was achieved from the intercept of the straight line. The K_d value of 5 orders of magnitude indicates that there exists a strong binding interaction between the two polyphenol inhibitors and LOX [1]. The values of K_d and n decreased as the temperature increased, which is in accordance with the K_{sv} and K_q values calculated before for the BCL and JSD binding to LOX. This result implies that the stability of the complex was reduced by the high temperature [30]. The K_d for BCL-LOX and JSD-LOX interactions were calculated to be 12.43 $\times$ 10^5 and 72.18 $\times$ 10^5 L/mol respectively at 298 K, which suggests that the binding capacity of LOX-JSD is stronger than that of LOX-BCL. This is consistent with the findings of fluorescence emission spectra analysis. Previous studies have shown that the interaction between native BSA and β-car was higher than the β-car/unfolded BSA interaction because it has higher K_d value, which confirms our conclusion that the combination of JSD and LOX is stronger [36]. The value of n (number of binding sites for the LOX-BCL and LOX-JSD complexes) were about equal to 1, indicating that JSD and BCL has a single binding site on LOX respectively. We have reported a similar conclusion obtained in our previous study demonstrating that chlorogenic acid has a single binding site with LOX [5].

3.5. Determination of thermodynamic parameters

It is well known that hydrophobic interactions, electrostatic forces, van der Waals forces, and hydrogen bonds can promote the combination of small molecules and biomolecules [31]. In order to explore the driving force behind LOX–BCL and LOX-JSD systems, the entropy change (ΔS), enthalpy change (ΔH) and free energy change (ΔG) were calculated by the Van't Hoff equations [26].

$$lnK_a = -\Delta H/RT + \Delta S/T \quad (4)$$

$$\Delta G = -RTlnK_a = \Delta H - T\Delta S \quad (5)$$

ΔG is the Gibbs free energy change, ΔH is the enthalpy change, ΔS is the entropy change, and T is the corresponding temperature (298 and 310 K), R is the gas constant (8.314 J mol^{-1} K^{-1}). Table 1 reveals that ΔG values were negative for both interactions, implying that the binding process was spontaneous. The negative values of ΔH and ΔS indicate that the binding process of BCL with LOX is mainly driven by the

Table 1
Quenching constant (K_{SV}), binding constant (K_d), quenching rate constant (K_q) and thermodynamic parameters of the LOX-JSD and LOX-BCL complexes at different temperatures.

	T (K)	K_{sv} (10^4 L/mol)	K_q (10^{12} L/mol·s)	K_d (10^5 L/mol)	n	△H (KJ/mol)	△S (J/mol·K)	△G (KJ/mol)
BCL	298	6.39	6.39	12.43	1.29	−66.11	−105.51	−34.77
	305	5.22	5.22	6.09	1.24			−33.78
	310	4.78	4.78	4.33	1.21			−33.45
JSD	298	9.78	9.78	72.18	1.41	−280.24	−809.42	−39.13
	305	6.62	6.62	4.88	1.19			−33.22
	310	5.27	5.27	0.89	1.05			−29.37

Note: n is the number of binding sites per protein, ΔS is the change in entropy, ΔH is the change in enthalpy and ΔG is the change in free energy.

hydrogen bond interaction and van der Waals force. The negative value of ΔH and the negative value of ΔS confirm that the hydrogen bond interaction and van der Waals force may play a major role in the binding process of the JSD-LOX system. These results are similar to earlier studies which reported that the combination of CGA (chlorogenic acid) and myofibrillar protein is due to the combination of hydrogen bonds and van der Waals forces [41].

3.6. Synchronous fluorescence spectral measurement

The synchronous fluorescence spectra can probe the changes in the molecular microenvironment near the Tyr and Trp residues of LOX during the procedure of BCL and JSD binding to LOX. The synchronous fluorescence spectra of LOX and LOX-polyphenols complex at specific intervals Δλ = 15 and 60 nm are illustrated in Fig. 1c–1d. After the addition of BCL, the maximum emission wavelength did not significantly shift with increasing BCL concentration for Δλ = 15 and 60 nm, while the fluorescence intensity gradually decreased. This indicates that BCL could quench the fluorescence of Trp and Tyr residues of LOX to form a stable complex with LOX, while the microenvironment of the Tyr residue and Trp residue failed to exhibit apparent changes for the combination of BCL and LOX [9]. For Δλ = 15 nm, the maximum emission wavelength is weakly blue-shifted (Fig. 1c1) with increasing concentration of JSD, but no shift is observed for Δλ = 60 nm, which demonstrates that the polarity around the tyrosine residues decreased, and hydrophobicity increased. This is consistent with the result of luteolin binding with xanthine oxidase, which showed that the hydrophobicity increased around tyrosine residues, while there was no significant change in the surrounding around tryptophan residues [43].

3.7. UV–vis absorption spectroscopy

UV–vis is widely used to explore and confirm the structural changes and complex formation during protein–ligand interactions. The UV–vis absorption spectra of LOX and LOX-polyphenols complexes were recorded and are displayed in Fig. 2a. There was a finding that the absorption of LOX around 275 nm gradually increased and generated a small blue shift following the increasing concentration of BCL and JSD. The results show that there exists an interaction between LOX and ligands as new complexes were created. Similar results were found during the interaction of eriocitrin with β-casein, the UV peak absorption intensity of β-casein at 280 nm increased after the addition of various doses of eriocitrin, which indicates the generation of eriocitrin-β-casein complex [6]. During the reaction and complex formation of polyphenols with LOX, a new characteristic absorption peak was also formed at 325 nm and 350 nm for BCL-LOX and JSD-LOX complexes, which can be attributed to the long wavelength charge transfer band between polyphenols and iron [27]. Some studies have also found that the characteristic peaks of polyphenols appear around 325–360 nm during the complexation process between polyphenols and proteins [50,48]. From Fig. 2a, it is obvious to see that both quenching styles of LOX and BCL or JSD are static quenching due to the dynamic quenching which only affects the excited state of the quenching molecule, and not the absorption spectra of the quenching substances. Previous studies have reported that the absorption spectra of the two carotene HSA/BSA systems are significantly different from those of HSA/BSA systems, which confirms that the role of static quenching [23].

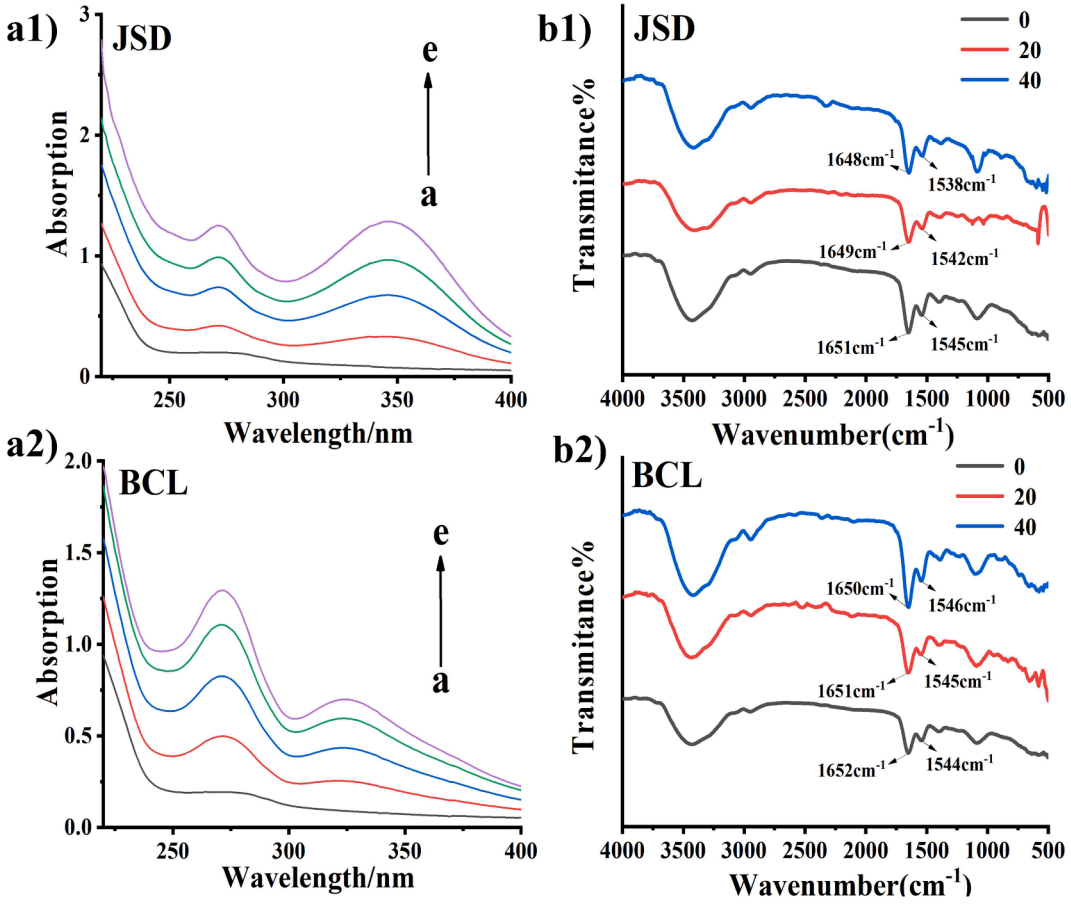

Fig. 2. UV–VIS/FT-IR spectra of JSD-LOX (a1 and b1) and BCL-LOX (a2 and b2) complex. Note: UV–VIS spectra of LOX with various concentrations of JSD (a1 a–e = 0, 10, 20, 30 and 40 × 10^{-6} mol/L) and BCL (a2 a–e = 0, 10, 20, 30 and 40 × 10^{-6} mol/L).

3.8. FT-IR spectra studies

The secondary structure changes of enzyme affected by polyphenols can be detected effectively with FT-IR spectroscopy. In these protein amide bands, both amide I band (1700–1600 cm^{-1}) and amide II band (1600–1500 cm^{-1}) have a strong relationship with protein secondary structure, amide I band which is mainly influenced by C═O stretch is more susceptible to changes in protein secondary structures compared with amide II band which is mainly influenced by C—N stretch coupled with N—H bending mode [38]. The FT-IR spectroscopy of LOX and LOX-polyphenols complexes are shown in Fig. 2b. The wavelength of amide I bands shifted from 1651 to 1648 cm^{-1} and 1652 to 1650 $cm^{-1}$when JSD and BCL were added to LOX respectively. The peak positions of the amide II band changed from 1545 to 1538 cm^{-1} and 1544 to 1546 cm^{-1} when JSD and BCL were added to LOX respectively. The results suggest that these two kinds of polyphenols interact with both the C═O and C—N groups in the peptide chain of protein, which results in changes of the LOX secondary structure [23]. The amide I and amide II bands have a larger displacement range after adding JSD illustrating that the addition of JSD significantly affects the secondary structure of LOX. Previous study reported that the binding of TFDG (theaflavin-3,3′-digallate) and BSA, as TFDG caused the destruction of the hydrogen bond network which ultimately led to changes in the secondary structure of BSA [46].

3.9. Particle size measurements

The determination of particle size can be used to explore the size distribution of LOX with or without polyphenols. The particle sizes of LOX with various doses of BCL and JSD are exhibited in Fig. 3. The average particle size of LOX was observed to be 611 ± 10 nm in solution. After the addition of polyphenols, the size of LOX complexes increased up to 988 ± 55 nm and 965 ± 25 nm for BCL-LOX and JSD-LOX systems, respectively. The reason may be that the conformation of LOX changed when BCL and JSD bound to LOX, allowing the hydrophobic interaction to result in protein combination [30]. A recent study showed that the size of the vitamin D3-α-lactalbumin complex was much larger than that of α-lactalbumin, suggesting that the addition of vitamin D3 brought about the exposure of hydrophobic plaques of α-lactalbumin, the hydrophobic interaction causes the formation of larger a-La complexes [11]. Cao et al. [5] studied the complexation of CGA with lipase, the addition of CGA caused aggregation of lipase and the increase in the average diameter of lipase indicated the formation of lipase-CGA complex.

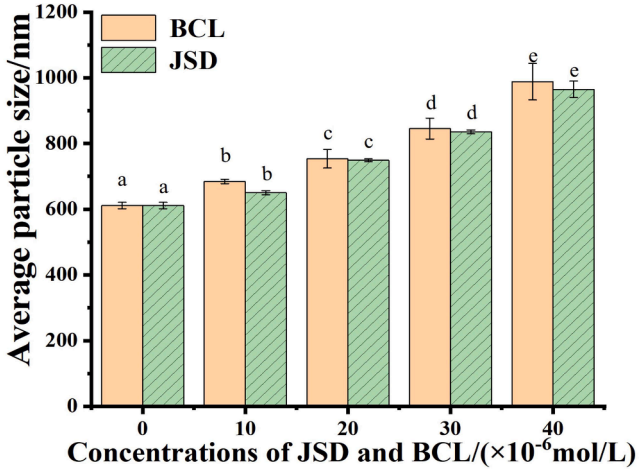

Fig. 3. Results of particle size analysis. Different lowercase letters (a, b, c, d and e) indicate significant differences in the average particle size values of the JSD–LOX or BCL–LOX complexes ($p < 0.05$).

3.10. AFM analysis

The properties of protein morphology may change if the protein structure is destroyed. AFM can probe the changes in LOX morphology during the interaction between LOX and polyphenols. The two and three dimensional images of LOX and LOX-polyphenol complexes are given in Fig. 4. LOX is uniformly adsorbed on the surface of mica, and its morphological image can be clearly observed in Fig. 4a. After adding polyphenols, it can be seen that the larger protein complex was created by the combination of small particles especially for JSD. This phenomenon confirms that the LOX-polyphenols complexes were formed [25]. The microenvironment around LOX becomes more hydrophobic when interacting with polyphenol. Therefore, LOX molecules minimize their surface area when they contact with water through molecular aggregation. A similar result was reported of the combination between the plant derived conferone and serum albumins [19].

3.11. Molecular docking study

Molecular docking is frequently used to foretell the apparent combination models for ligands and proteins. In this study, the molecular docking project aimed to identify the major binding sites for LOX binding to polyphenols and the amino acid residues that interact with polyphenols. The findings of molecular docking are shown in Fig. 5a–5c. It can be observed that a variety of hydrogen bonds have been established between BCL and LOX (Fig. 5c2), the hydroxyl group on the ring of BCL formed aromatic hydrogen bond with the aromatic hydrocarbon in the sidechain of His366 (Bond length: 3.62 Å) in LOX, the other two hydroxyl groups, hydrogen bond donors, formed conventional hydrogen bond with the oxygen atom in the sidechain of Ile663 (Bond length: 4.05 Å and 4.49 Å, respectively). Furthermore, Van Der Waals' force dominates the role in BCL-LOX system interaction as displayed in Fig. 5c2. The results above showed that hydrogen bonds and van der Waals forces mainly stimulate the combination of LOX and BCL, which are consistent with the thermodynamic analysis. As shown in Fig. 5c1, JSD formed more hydrogen bonds with LOX, including the conventional hydrogen bond with l-isoleucine (Ile) 593 (3.37 Å) and aspartic (ASN) 401 (3.12 Å), carbon hydrogen bonds with glutamic acid (Glu) 357 (5.44 Å and 4.33 Å) and l-isoleucine (Ile) 663 (5.20 Å). These hydrogen bonds stabilize the spatial conformation of polyphenols and LOX complexes [30]. The benzene ring of JSD formed hydrophobic interactions with Ala 404 (5.02 Å), isoleucine (Ile) 593 (6.14 Å), Leu 362 (5.43 Å) and Leu 408 (5.46 Å and 5.26 Å). The formation of these hydrophobic bonds helps maintain the three-dimensional structure of the JSD-LOX complex. Additionally, it was noted that the interaction between apigenin and PPO molecules is comparable to the result [42]. Docking analysis showed that the minimum binding affinity is JSD-LOX (−5.8 kJ/mol) > BCL-LOX (−3.7 kJ/mol), which also proved that JSD has a stronger binding affinity with LOX. However, the bond length of JSD binding with LOX is shorter, so the n value of JSD decreases sharply with increasing temperature(1.41–1.05), indicating that the stability of the binding site of JSD with LOX is poorer at high temperature. The molecular docking findings have proved that the hydrogen bond formed between JSD, and LOX is more evenly distributed due to the slight structural difference between the two LOX inhibitors (the groups forming hydrogen bonds with LOX on JSD are more dispersed than that of BCL), which leads to a closer combination between JSD and LOX. A previous study found that paclitaxel has more benzene rings and hydroxyl groups than artemisinin, which leads to a greater effect of paclitaxel on the structural changes of BSA [29].

3.12. Molecular dynamic simulation

Molecular dynamics simulation is very important when the stability and dynamic behavior of ligand and protein complexes were studied. Herein, root mean square deviations (RMSD), and root mean square

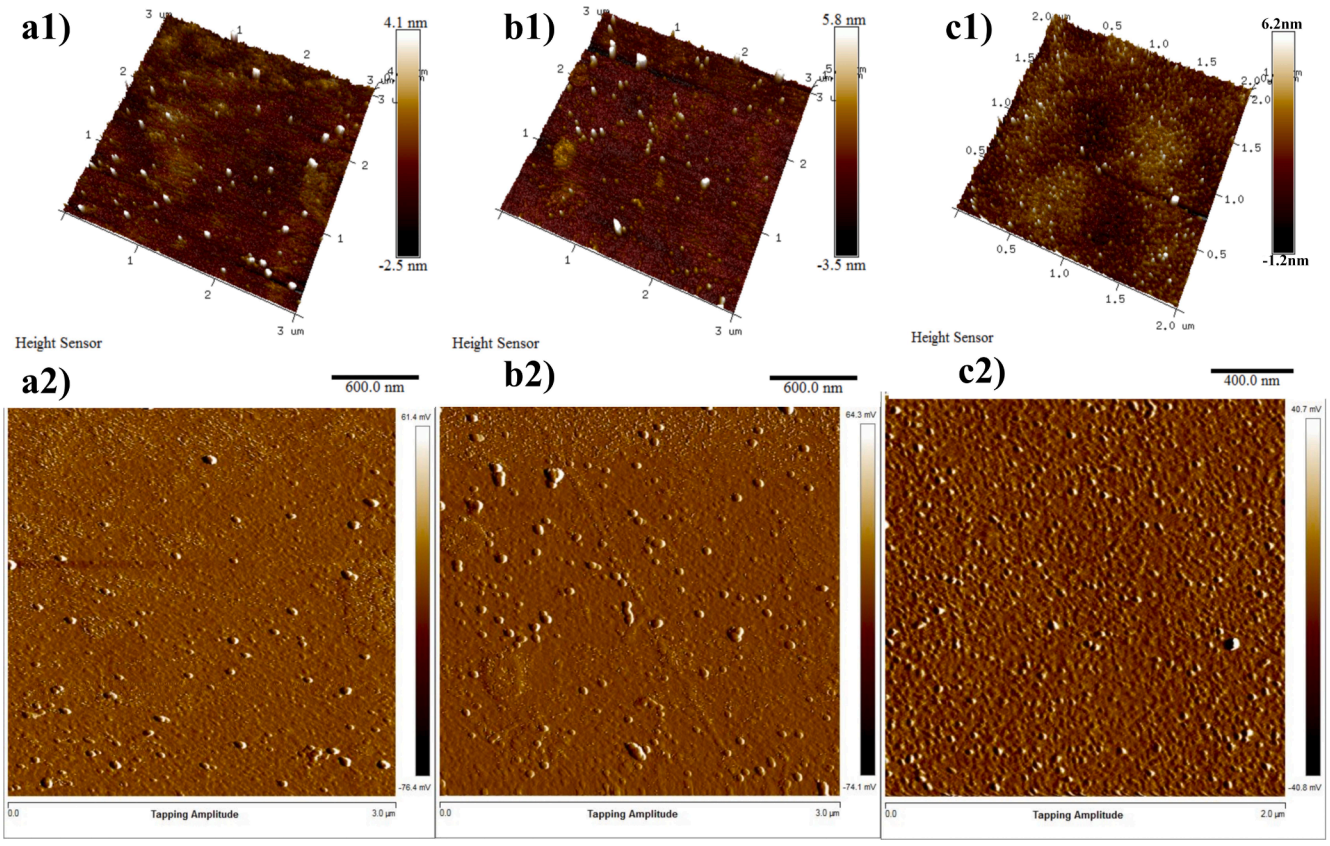

Fig. 4. (a1) AFM three-dimensional topography image of LOX. (b1) AFM three-dimensional topography image of BCL-LOX complex. (c1) AFM three-dimensional topography image of JSD-LOX complex. (a2, b2 and c2) are the topography graph for (a1, b1 and c1), respectively.

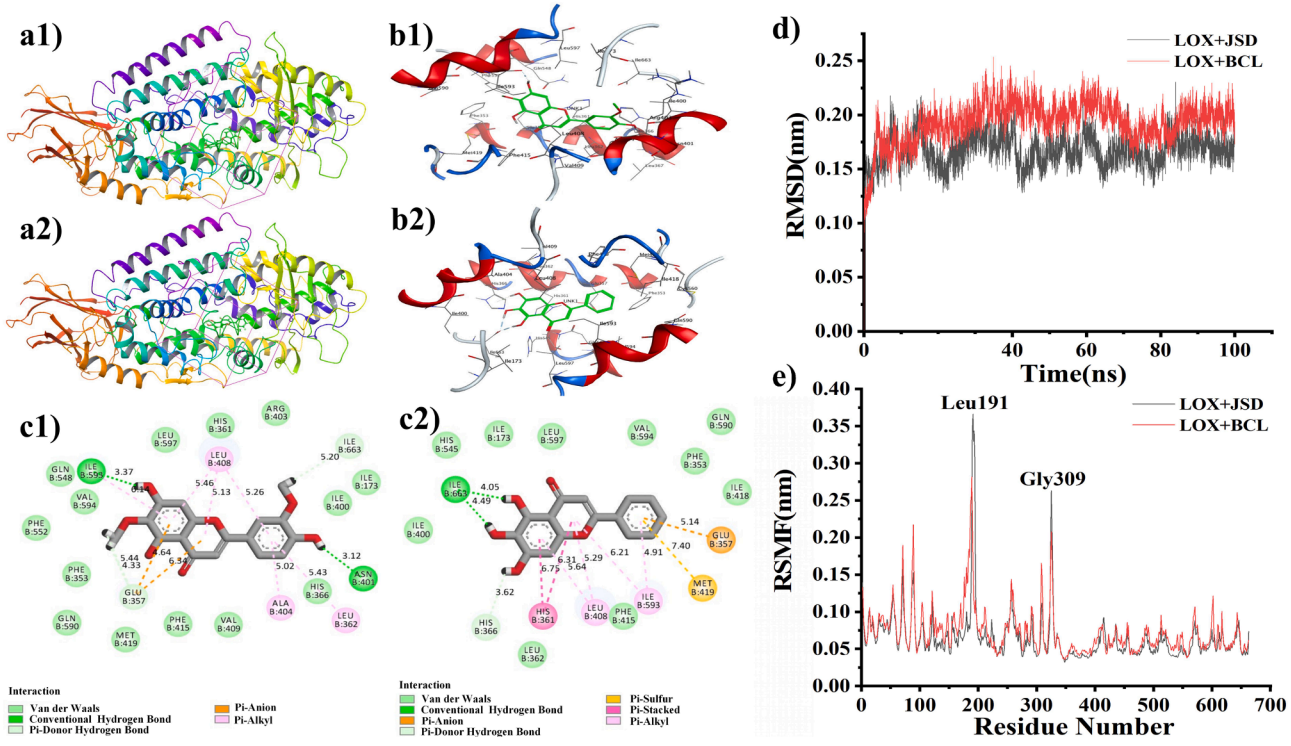

Fig. 5. Results of molecular docking and molecular simulation of JSD-LOX and BCL-LOX complex. Note: (a): Docking ligand at the binding site. (b) Results of 3D molecular docking modeling; (c) results of 2D molecular docking modeling. Profiles of the molecular dynamics simulations: (d) RMSD values for the JSD-LOX complexes (black) and BCL–LOX complexes (red); (e) RMSF values of the JSD–LOX complexes (black) and BCL–LOX complexes (red).

fluctuations (RMSF) were analyzed to evaluate the conformational changes of LOX during the binding process. The findings revealed that the RMSD value of the LOX-polyphenol complexes structure fluctuated greatly within 20–80 ns (Fig. 5d). Overall structures of the LOX-JSD and LOX-BCL systems reached equilibrium after 100 ns. However, the RMSD value of the LOX-JSD complex was smaller than that of the LOX-BCL complex. That means the LOX-JSD complex is more stable than the LOX-BCL one, which is similar to the results of molecular docking analysis. The time averaged root mean square fluctuations (RMSF) of protein residues was obtained to analyze position variation of particles and local changes in the protein structure. The results of RMSF calculation in Fig. 5e. showed that the RMSF value of the LOX-BCL complex was generally greater than the RMSF value of the LOX-JSD complex, indicating that the combination of JSD can restrict the fluctuation of LOX more. An earlier study found that the RMSD value of HAS decreased after the addition of corilagin which suggests that the process of the ligand binds to protein increases the rigidity and stability of the structure [45]. However, the high fluctuation region of the LOX-JSD complex appeared in the following residue range: 180–200 and 320–330. The amino acid residues in this region such as Leucine (Leu) 191 and Glycine (Gly) 309 are essentially in the region where JSD and LOX bond. Given that the structure of brown cyanidin is more complex than that of scutellarin, brown cyanidin has a higher effect on the structural change of LOX when combined with LOX.

4. Conclusions

The interaction mechanisms of BCL-LOX and or JSD-LOX systems were explored by using multi-spectroscopic and computational study. The intrinsic fluorescence intensity of LOX is significantly quenched by JSD and BCL mainly through static quenching. The binding constant of LOX-JSD and LOX-BCL indicates that LOX has stronger binding affinity to JSD compared to BCL. The docking simulation results demonstrate that there are more hydrogen bonds in the JSD–LOX system and the hydrogen bonds are more evenly distributed, resulting in a tighter bond formed between JSD and LOX. The molecular dynamic simulation results show that the complex formed by LOX and JSD is more stable, and the addition of JSD is more conducive to the formation of complex molecules. This study provides some theoretical basis for the inhibitory mechanism of polyphenols on LOX, and expects to afford some useful information on the preservation of aquatic products.

Funding declaration

This research was financially supported by the National Natural Science Foundation of China (No. 31772047) and the National Key R & D Program of China (No. 2019YFC1606003).

CRediT authorship contribution statement

Zeru Xu: Methodology, Formal analysis, Writing - original draft. **Hongying Du:** Methodology, Supervision, Conceptualization, Formal analysis, Funding acquisition, Writing - review & editing. **Anne Manyande:** Writing – review & editing.

Declaration of Competing Interest

The authors declare that they have no known competing financial interests or personal relationships that could have appeared to influence the work reported in this paper.

Data availability

Data supporting the findings of this study are available upon request from the corresponding author.

Appendix A. Supplementary data

Supplementary data to this article can be found online at https://doi.org/10.1016/j.saa.2023.123423.

References

[1] M.I. Ahmad, A.M. Potshangbam, M. Javed, M. Ahmad, Studies on conformational changes induced by binding of pendimethalin with human serum albumin, Chemosphere 243 (2020), 125270.
[2] G. Began, E. Sudharshan, A.G.A. Rao, Inhibition of lipoxygenase 1 by phosphatidylcholine micelles-bound curcumin, Lipids 33 (12) (1998) 1223.
[3] B. Bie, J. Sun, Y. Guo, J. Li, W. Jiang, J. Yang, C. Huang, Z. Li, Baicalein: a review of its anti-cancer effects and mechanisms in Hepatocellular Carcinoma, Biomed. Pharmacother. 93 (2017) 1285–1291.
[4] Q. Cao, H. Du, Y. Huang, Y. Hu, J. You, R. Liu, S. Xiong, A. Manyande, The inhibitory effect of chlorogenic acid on lipid oxidation of grass carp (*Ctenopharyngodon idellus*) during chilled storage, Food Bioproc. Technol. 12 (12) (2019) 2050–2061.
[5] Q. Cao, Y. Huang, Q.-F. Zhu, M. Song, S. Xiong, A. Manyande, H. Du, The mechanism of chlorogenic acid inhibits lipid oxidation: an investigation using multi-spectroscopic methods and molecular docking, Food Chem. 333 (2020), 127528.
[6] X. Cao, Y. He, Y. Kong, X. Mei, Y. Huo, Y. He, J. Liu, Elucidating the interaction mechanism of eriocitrin with β-casein by multi-spectroscopic and molecular simulation methods, Food Hydrocoll. 94 (2019) 63–70.
[7] D.A. Case, T.E. Cheatham 3rd, T. Darden, H. Gohlke, R. Luo, K.M. Merz Jr., A. Onufriev, C. Simmerling, B. Wang, R.J. Woods, The Amber biomolecular simulation programs, J. Comput. Chem. 26 (16) (2005) 1668–1688.
[8] T.-t. Chai, Y.-n. Huang, S.-t. Ren, D.-l. Jin, J.-j. Fu, G. J-y, Y.-w. Chen, Inhibitory effects of ultrasonic and rosmarinic acid on lipid oxidation and lipoxygenase in large yellow croaker during cold storage, Ultrason. Sonochem. 92 (2023), 106229.
[9] R. Chen, Y. Shi, G. Liu, Y. Tao, Y. Fan, X. Wang, L. Li, Spectroscopic studies and molecular docking on the interaction of delphinidin-3-O-galactoside with tyrosinase, Biotechnol. Appl. Biochem. 69 (4) (2021) 1327–1338.
[10] D.-S. Chou, J.-J. Lee, G. Hsiao, C.-Y. Hsieh, Y.-J. Tsai, T.-F. Chen, J.-R. Sheu, Baicalein induction of hydroxyl radical formation via 12-lipoxygenase in human platelets: an ESR study, J. Agric. Food Chem. 55 (3) (2007) 649–655.
[11] B. Delavari, A.A. Saboury, M.S. Atri, A. Ghasemi, B. Bigdeli, A. Khammari, P. Maghami, A.A. Moosavi-Movahedi, T. Haertlé, B. Goliaei, Alpha-lactalbumin: a new carrier for vitamin D3 food enrichment, Food Hydrocoll. 45 (2015) 124–131.
[12] R.A. Friesner, J.L. Banks, R.B. Murphy, T.A. Halgren, J.J. Klicic, D.T. Mainz, M. P. Repasky, E.H. Knoll, M. Shelley, J.K. Perry, D.E. Shaw, P. Francis, P.S. Shenkin, Glide: a new approach for rapid, accurate docking and scoring. 1. Method and assessment of docking accuracy, J. Med. Chem. 47 (7) (2004) 1739–1749.
[13] R.A. Friesner, R.B. Murphy, M.P. Repasky, L.L. Frye, J.R. Greenwood, T.A. Halgren, P.C. Sanschagrin, D.T. Mainz, Extra precision glide: docking and scoring incorporating a model of hydrophobic enclosure for protein-ligand complexes, J. Med. Chem. 49 (21) (2006) 6177–6196.
[14] J.L. Gata, M.C. Pinto, P. Macias, Lipoxygenase activity in pig muscle: purification and partial characterization, J. Agric. Food Chem. 44 (9) (1996) 2573–2577.
[15] J. Gu, S. Zheng, X. Huang, Q. He, T. Sun, Exploring the mode of binding between butylated hydroxyanisole with bovine serum albumin: multispectroscopic and molecular docking study, Food Chem. 357 (2021), 129771.
[16] P. Han, N. An, L. Yang, X. Ren, S. Lu, H. Ji, Q. Wang, J. Dong, Molecular dynamics simulation of the interactions between sesamol and myosin combined with spectroscopy and molecular docking studies, Food Hydrocoll. 131 (2022), 107801.
[17] J. Hong, C.S. Yang, Effects of tea polyphenols on arachidonic acid metabolism in human colon, in: Food Factors in Health Promotion and Disease Prevention, Vol. 851. ACS Symposium Series, Vol. 851, American Chemical Society, 2003, pp. 27–38.
[18] Y. Huang, H. Du, G.M. Kamal, Q. Cao, C. Liu, S. Xiong, A. Manyande, Q. Huang, Studies on the binding interactions of grass carp (*Ctenopharyngodon idella*) myosin with chlorogenic acid and rosmarinic acid, Food Bioproc. Technol. 13 (8) (2020) 1421–1434.
[19] L. Khalili, G. Dehghan, A comparative spectroscopic, surface plasmon resonance, atomic force microscopy and molecular docking studies on the interaction of plant derived conferone with serum albumins, J. Lumin. 211 (2019) 193–202.
[20] J. Kongsted, U. Ryde, An improved method to predict the entropy term with the MM/PBSA approach, J. Comput. Aided Mol. Des. 23 (2) (2009) 63–71.
[21] R. Landberg, K. Sunnerheim, L.H. Dimberg, Avenanthramides as lipoxygenase inhibitors, Heliyon 6 (6) (2020), e04304.
[22] C.A. Lelis, D. Galvan, C.A. Conte-Junior, Nanocarriers for β-carotene based on milk protein, Food Bioproc. Technol. (2022).
[23] X. Li, G. Wang, D. Chen, Y. Lu, β-carotene and astaxanthin with human and bovine serum albumins, Food Chem. 179 (2015) 213–221.
[24] W. Lv, X. Sheng, T. Chen, Q. Xu, X. Xie, Jaceosidin induces apoptosis in human ovary cancer cells through mitochondrial pathway, J. Biomed. Biotechnol. 2008 (2008), 394802.
[25] Y. Lv, Q. Liang, Y. Li, X. Liu, D. Zhang, X. Li, Study of the binding mechanism between hydroxytyrosol and bovine serum albumin using multispectral and molecular docking, Food Hydrocoll. 122 (2022), 107072.

[26] H. Ma, T. Zou, H. Li, H. Cheng, The interaction of sodium dodecyl sulfate with trypsin: multi-spectroscopic analysis, molecular docking, and molecular dynamics simulation, Int. J. Biol. Macromol. 162 (2020) 1546–1554.
[27] M.J. Nelson, Catecholate complexes of ferric soybean lipoxygenase 1, Biochemistry 27 (12) (1988) 4273–4278.
[28] M. Nikpour, M. Mousavian, M. Davoodnejad, M. Alimardani, H. Sadeghian, Synthesis of new series of pyrimido[4,5-b][1,4] benzothiazines as 15-lipoxygenase inhibitors and study of their inhibitory mechanism, Med. Chem. Res. 22 (10) (2013) 5036–5043.
[29] H. Qi, Y. Wang, X. Wang, L. Su, Y. Wang, S. Wang, The different interactions of two anticancer drugs with bovine serum albumin based on multi-spectrum method combined with molecular dynamics simulations, Spectrochim. Acta A: Mol. Biomol. Spectrosc. 259 (2021), 119809.
[30] X. Qi, D. Xu, J. Zhu, S. Wang, J. Peng, W. Gao, Y. Cao, Studying the interaction mechanism between bovine serum albumin and lutein dipalmitate: multi-spectroscopic and molecular docking techniques, Food Hydrocoll. 113 (2021), 106513.
[31] L. Roufegarinejad, A. Jahanban-Esfahlan, S. Sajed-Amin, V. Panahi-Azar, M. Tabibiazar, Molecular interactions of thymol with bovine serum albumin: spectroscopic and molecular docking studies, J. Mol. Recognit. 31 (7) (2018), e2704.
[32] T. Sae-leaw, S. Benjakul, Fatty acid composition, lipid oxidation, and fishy odour development in seabass (*Lates calcarifer*) skin during iced storage, Eur. J. Lipid Sci. Technol. 116 (7) (2014) 885–894.
[33] R. Salomon-Ferrer, D.A. Case, R.C. Walker, An overview of the Amber biomolecular simulation package, WIREs Comput. Mol. Sci. 3 (2) (2013) 198–210.
[34] D. Saul, S. Gleitz, H.H. Nguyen, R.L. Kosinsky, S. Sehmisch, D.B. Hoffmann, M. Wassmann, B. Menger, M. Komrakova, Effect of the lipoxygenase-inhibitors baicalein and zileuton on the vertebra in ovariectomized rats, Bone 101 (2017) 134–144.
[35] K. Sekiya, H. Okuda, Selective inhibition of platelet lipoxygenase by baicalein, Biochem. Biophys. Res. Commun. 105 (3) (1982) 1090–1095.
[36] C.E.L. Silva, E.A. Hudson, A.J.P. Agudelo, L.H.M. Da Silva, M.S. Pinto, D.C. H. Maria, F.A.R. Barros, A.C. Clarissa, β-carotene and milk protein complexation: a thermodynamic approach and a photo stabilization study, Food Bioprocess Technol. (2018).
[37] Q. Song, S. Peng, X. Zhu, Baicalein protects against MPP+/MPTP-induced neurotoxicity by ameliorating oxidative stress in SH-SY5Y cells and mouse model of Parkinson's disease, Neurotoxicology 87 (2021) 188–194.
[38] H. Tang, F. Ma, D. Zhao, Integrated multi-spectroscopic and molecular modelling techniques to probe the interaction mechanism between salvianolic acid A and α-glucosidase, Spectrochim. Acta A: Mol. Biomol. Spectrosc. 218 (2019) 51–61.
[39] Ş. Tolasa Yılmaz, Ş. Çaklı, E.B. Şen Yılmaz, F. Kırlangıç, C. Lee, Effect of fillet temperature on lipoxygenase activity in sardine mince with and without milk protein concentrate, LWT 90 (2018) 38–44.
[40] S.M. Woo, T.K. Kwon, Jaceosidin induces apoptosis through Bax activation and down-regulation of Mcl-1 and c-FLIP expression in human renal carcinoma Caki cells, Chem. Biol. Interact. 260 (2016) 168–175.
[41] W. Xie, Y. Huang, Y. Xiang, S. Xiong, A. Manyande, H. Du, Insights into the binding mechanism of polyphenols and fish myofibrillar proteins explored using multi-spectroscopic methods, Food Bioproc. Technol. 13 (5) (2020) 797–806.
[42] Z. Xiong, W. Liu, L. Zhou, L. Zou, J. Chen, Mushroom (*Agaricus bisporus*) polyphenoloxidase inhibited by apigenin: multi-spectroscopic analyses and computational docking simulation, Food Chem. 203 (2016) 430–439.
[43] J. Yan, G. Zhang, Y. Hu, Y. Ma, Effect of luteolin on xanthine oxidase: inhibition kinetics and interaction mechanism merging with docking simulation, Food Chem. 141 (4) (2013) 3766–3773.
[44] P.S. Yashaswini, A.G.A. Rao, S.A. Singh, Inhibition of lipoxygenase by sesamol corroborates its potential anti-inflammatory activity, Int. J. Biol. Macromol. 94 (2017) 781–787.
[45] D.P. Yeggoni, A. Rachamallu, R. Subramanyam, A comparative binding mechanism between human serum albumin and α-1-acid glycoprotein with corilagin: biophysical and computational approach, RSC Adv. 6 (46) (2016) 40225–40237.
[46] X. Yu, X. Cai, S. Li, L. Luo, J. Wang, M. Wang, L. Zeng, Studies on the interactions of theaflavin-3,3′-digallate with bovine serum albumin: Multi-spectroscopic analysis and molecular docking, Food Chem. 366 (2022), 130422.
[47] H.-j. Zeng, J. You, R. Yang, L.-b. Qu, Molecular interaction of silybin with hyaluronidase: a spectroscopic and molecular docking study, Spectrosc. Lett. 50 (10) (2017) 515–521.
[48] Y. Zhang, Y. Lu, Y. Yang, S. Li, C. Wang, C. Wang, T. Zhang, Comparison of non-covalent binding interactions between three whey proteins and chlorogenic acid: spectroscopic analysis and molecular docking, Food Biosci. 41 (2021), 101035.
[49] X. Zhou, D.-Y. Zhou, Z.-Y. Liu, F.-W. Yin, Z.-Q. Liu, D.-Y. Li, F. Shahidi, Hydrolysis and oxidation of lipids in mussel *Mytilus edulis* during cold storage, Food Chem. 272 (2019) 109–116.
[50] J. Zhu, Z. Li, C. Wu, G. Fan, T. Li, D. Shen, J. Dou, Y. Liang, Insight into the self-assembly behavior of α-zein by multi-spectroscopic and molecular simulations: an example of combination with the main component of jujube peel pigments – Rutin, Food Chem. 404 (2023), 134684.
[51] P. Cieplak, W.D. Cornell, C. Bayly, P.A. Kollman, Application of the multimolecule and multiconformational RESP methodology to biopolymers: Charge derivation for DNA, RNA, and proteins, J Comput Chem 16 (11) (1995) 1357–1377, https://doi.org/10.1002/jcc.540161106.